Colloid Polym Sci (2005) 283: 1025–1032
DOI 10.1007/s00396-004-1265-2

Parnia Navabpour
Carlos Rega
Christopher J. Lloyd
David Attwood
Peter A. Lovell
Pauline Geraghty
David Clarke

Influence of concentration on the particle size analysis of polymer latexes using diffusing-wave spectroscopy

Received: 6 April 2004
Accepted: 6 December 2004
Published online: 2 April 2005

C. Rega · C. J. Lloyd
D. Attwood · D. Clarke
School of Pharmacy and Pharmaceutical Sciences, University of Manchester, Oxford Rd, Manchester, M13 9PL, UK

P. Navabpour · P. A. Lovell
Manchester Materials Science Centre, UMIST, Grosvenor St., Manchester, M1 7HS, UK

P. Geraghty
GlaxoSmithKline, New Frontiers Science Park (South), Third Ave, Harlow, Essex, CM19 5AW, UK

Present address: C. Rega (✉)
Malvern Instruments, Enigma Business Park, Grovewood Road, Malvern, WR14 1XZ, UK
E-mail: carlos.rega@malvern.co.uk
Tel.: + 44 (0)1684 892456
Fax: +44 (0) 1684 892789

P. Navabpour
IPTME, Loughborough University, Loughborough, LE11 3TU, UK

Present address: P. Navabpour
Teer Coatings Ltd, Droitwich, WR9 9AS, UK

Abstract The use of a diffusing-wave spectroscopy (DWS) technique for the particle size analysis of a series of suspensions of polymer latexes with diameters ranging between 90 nm and 1300 nm and volume fractions from 0.02 to 0.18 has been investigated. Particle sizes from DWS were in reasonable agreement with those from transmission electron microscopy and disc centrifuge photosedimentometry. Photon correlation spectroscopy was applicable only to the latexes with particle sizes less than 500 nm. For polymer latexes with volume fractions (V_f) up to 0.09, the decay rate of the autocorrelation function from DWS was related to the particle size over the range of particle sizes examined. At the highest volume fraction (V_f = 0.18), it was possible to distinguish between particles with diameters of 740 and 1,300 nm from their autocorrelation functions, but not between particles with diameters of 90 and 430 nm.

Introduction

Photon correlation spectroscopy (PCS) has been extensively used to study the internal structure of colloid and polymer systems [1, 2]. In a classical PCS experiment, the light scattered by the sample is collected by a photomultiplier and the signal produced by the photomultiplier is analysed using an auto-correlator. The resulting autocorrelation function (ACF), can then be analysed to obtain, for instance, the particle size and particle-size distribution of the system. However, the theoretical models used to calculate the particle size are only valid in the single scattering regime, and consequently, PCS can usually only be used in dilute systems.

In the late 1980s an extension of the principles of PCS to concentrated highly-scattering media, was introduced [3, 4]. In this technique, known as diffusing-wave spectroscopy (DWS), the propagation of light through a highly scattering medium is treated as a diffusion process, and the ACF of the scattered light can be calculated theoretically. The theoretical expression obtained for the ACF can then be used to extract information about the internal dynamics of the system from the scattering data.

Maret and Wolf [3] observed that in the diffusion approximation, the ACF of the scattered intensity of light can be written as follows

$$G_1(\tau) \propto \int_0^\infty P(s) \exp[-(2\tau/\tau_0)(s/l^*)]\mathrm{d}s \quad (1)$$

where τ is the correlation time, τ_0 is the characteristic time of the diffusion of the particles in the medium, $P(s)$ is the probability of a photon travelling along a path of length s inside the medium and l^* is the distance over which the light has to travel into the medium before its propagation can be considered diffusive. Pine et al. [4] observed from Eq 1 that $G_1(\tau)$ is the Laplace transform of $P(s)$, and hence the normalised intensity ACF can be written as:

$$g_1(\tau) = \frac{\bar{U}(\vec{r},\tau)}{\bar{U}(\vec{r},0)} \quad (2)$$

where $\bar{U}$ is the Laplace transform of the energy density of light and $\vec{r}$ is the position at which the scattered light is observed.

In the diffusion approximation, U is calculated by solving the diffusion equation with the initial and boundary conditions appropriate to the geometry of the experiment. In general, it is found that the ACF obtained by this approximation has a much faster decay than the ACF obtained for a PCS experiment, in agreement with previous experimental observations [5]. While the ACF from PCS shows an exponential decay with the correlation time, the ACF obtained for a DWS experiment shows an exponential decay time with the square root of the correlation time, as shown in Eq. 3.

$$g_1(\tau) \propto \exp[-\sqrt{\tau/\tau_0}] \quad (3)$$

The faster decay of the ACF in the high scattering limit is expected, since each photon undergoes a large number of scattering events before being detected, and consequently the phase changes occur more rapidly than in the PCS case.

In a previous paper [6] an optical-fibre based DWS probe using back-scattering geometry was presented and used to determine differences in the particle size of latex standards with a 2.5% solids content. The purpose in designing the DWS probe presented in that paper was to develop a qualitative method for comparing particle sizes of concentrated, highly scattering systems. This paper presents a study of the effect of sample concentrations on the ability of the DWS probe to follow size changes qualitatively using narrow particle size distribution latexes.

Experimental

Latex preparation

Materials

Methyl methacrylate (MMA), butyl acrylate (BA), ammonium persulfate (APS) and azobisisobutyronitrile (AIBN) were obtained from Aldrich. The sodium dodecylbenzenesulfonate (SDBS) was obtained from Sigma. In order to remove the inhibitor, MMA and BA were washed three times with equal amounts of 2% aqueous sodium hydroxide in a separating funnel and then several times with water. They were subsequently kept over anhydrous calcium chloride to dry. All the other chemicals were used as received without further purification.

Polymerisation

MMA/BA (63.7/36.3 by weight) copolymer particles were prepared at 30 wt% solids by a semi-continuous emulsion polymerisation process at 80°C, using the procedures described by O'Callaghan et al. [7] modified slightly by not using the chain transfer agent. The formulations of the reactions are given in Table 1. In reaction R1, SDBS (0.10 g) was dissolved in water

Table 1 Formulations used for the preparation of the latex samples

Formulation		Reaction code			
		R1	R2	R3	R4
Precharge	Seed	–	–	R1	R2
	Amt seed	–	–	100	100
	Deionised water	350	350	100	100
	APS	1.00	1.00	–	–
	AIBN	–	–	0.05	0.05
	SDBS	0.10	–	–	–
Continuous feed	MMA	95.55	95.55	95.55	95.55
	BA	54.45	54.45	54.45	54.45
	AIBN	–	–	1.00	1.00
	SDBS	–	–	0.15	0.15
	Deionised water	–	–	250	250

All the amounts are given in grams

(300 g) and the solution was charged in a round-bottomed flask, which was placed in a water bath at 80°C and heated to the reaction temperature with stirring, under flowing nitrogen. APS (1 g) dissolved in water (20 g) was then added to the flask and the monomer mixture consisting of MMA (95.55 g) and BA (54.45 g) was fed to the flask using a peristaltic pump at a rate of 0.75 ml min^{-1}. The reaction was allowed to proceed for 2 h after the addition of the monomer was completed. Reactions R2, R3 and R4 were carried out in a similar manner, but without the addition of SDBS. The product of R2 was used as the seed for R3, and R3 was used as the seed for R4. For each of the reactions R3 and R4, the appropriate seed (100 g) and water (100 g) were added to the reaction flask, purged with nitrogen and heated to the reaction temperature. A surfactant solution was made by dissolving SDBS (15 g) in water (250 g). The MMA (95.55 g), BA (54.45 g) and AIBN (0.95 g) were mixed and added to the surfactant solution under constant stirring to form a pre-emulsion. Prior to the start of polymerisation, AIBN (0.05 g) was added to the reaction flask and the pre-emulsion was then added at a rate of 1.1 ml min^{-1}. The reaction was allowed to proceed for 1–2 h after the addition of the pre-emulsion was completed.

Monomer conversions in all reactions were analysed using gas liquid chromatography by measuring the amount of unreacted monomer at the end of the reactions. In each case the final conversions were greater than 98%.

Particle-size characterisation

Diffusing-wave spectroscopy (DWS) measurements

Four suspensions with solids contents of 20, 10, 5 and 2.5 wt% (volume fractions = 0.18, 0.09, 0.04 and 0.02, respectively) were prepared from each of the latex samples. DWS measurements were performed on each using the point source back-scattering DWS probe described in [6]. This probe is designed to exclude single and low order scattering events by both excluding scattered light polarised in the same plane as the incident light, and geometrically excluding paths shorter than l^*. The experimental arrangement for the measurements is shown in Fig. 1: fibre (Fig. 1a) is coupled to a laser module (532 nm wavelength, 100 mW power output, supplied by Laser 2000), and is used to illuminate the sample; and fibre (Fig. 1b) collects the light scattered by the sample, which is sent to an EMI Model P30CWAD5-10 photomultiplier connected to a Correlator.com Model FLEX99012C correlator. A 2 cm diameter sample cell was used, with a sample height of 2 cm.

For each sample, an average of 12 measurements of the ACF, with a measurement duration of 60 s, was determined. The error for each correlation point was obtained as the standard deviation of the average.

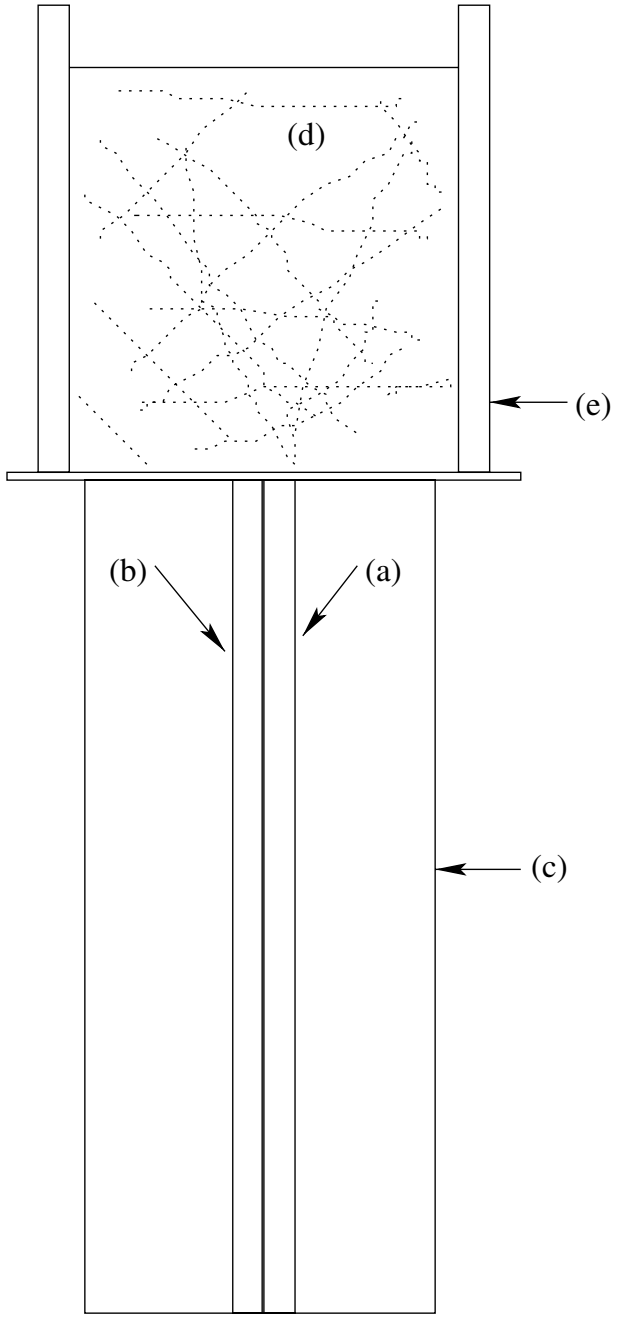

Fig. 1 Diagrammatical representation of the DWS probe head and sample cell. **a** and **b** are optical fibres (125 μm diameter each) for input of incident light and collection of scattered light. **c** probe body (1.6 cm diameter, 12 cm length). **d** sample. **e** sample cell (2 cm diameter, 2.5 cm height). The sizes of the elements are not to scale

The theoretical ACF for the DWS instrument used is as follows [6]

$$g_2(\tau) = P_1 + P_2 \times \left[\frac{1 + \left[6\gamma \Big/ \left(2(6\tau/\tau_0)^{1/2} + 3\right)^2\right]}{1 + (2\gamma/3)}\right]^2 \exp\left[-2\gamma(6\tau/\tau_0)^{1/2}\right], \quad (4)$$

where γ is a calibration constant, τ is the correlation time, P_1 is the ACF baseline and P_2 is the intercept of the ACF.

In theory, P_1 should be equal to 1, but small amounts of noise can change its value slightly, and assuming that the baseline is unity might change the estimates of the remaining parameters [8], for that reason we treat the baseline as an adjustable parameter. P_2 should also be unity, however, in our case—probably due to misalignment of the polarisation axes of the optical fibres—it was necessary to treat the intercept as an adjustable parameter.

For each of the concentrations, the calibration constant γ (as well as the parameters $P_1$and P_2) is calculated by fitting the experimental ACF for R4 to Eq. 4 with the Levenberg–Marquardt non-linear least squares method [9]. For each of the concentrations the value of τ_0 for R4 is calculated using the following expression derived from the Stokes–Einstein relationship:

$$\tau_0 = \frac{6\eta R_h \lambda^2}{4\pi k_B T n^2}, \quad (5)$$

where η is the viscosity of the suspension, R_h is the hydrodynamic radius of the particles, λ the wavelength of the illuminating laser, k_B the Boltzmann constant, T the temperature at which the experiment is performed and n the refractive index of the suspension.

The viscosities of the R4 sample at each concentration were measured using a U-tube viscometer. The refractive index was measured with an Abbé 60/ED precision refractometer (Bellingham and Stanley Ltd.). In the systems under investigation the viscosity of the suspension rather than that of the solvent was used, because in concentrated suspensions each particle can be considered to "see" an effective medium equivalent to the suspension [10]. The value used for the hydrodynamic radius is the z-average as obtained from DCP measurements, which accounts for the changes in scattering efficiency with particle size [11].

Once the value of the calibration constant γ has been calculated for each concentration, the values of τ_0 for the products of R1, R2 and R3 are obtained by fitting the experimental data to Eq. 4 with the value of γ obtained in the calibration step, and allowing P_1, P_2 and τ_0 to float.

In this study it is assumed that γ is only affected by the concentration of the sample, given identical samples. From the theory of DWS, γ is mainly a geometric factor determined by the distance l^* that the light needs to travel into the sample before its propagation can be considered diffusive [5, 6, 12, 13]. It is a reasonable assumption then, that as long as the detected light travels a distance significantly longer than l^*, γ is mainly a function of concentration. However, to account for additional effects that would be contained in the value of τ_0 obtained using γ as a calibration constant, we use $\sqrt{\tau_0}/\gamma$ as the size-correlated parameter.

Photon correlation spectroscopy (PCS) measurements

The particle sizes of latexes were analysed using a Brookhaven laser light scattering instrument equipped with a 20 mW HeNe laser and a BI-9000AT digital correlator. Analyses were carried out at 25 ± 0.1°C for a period of 10 min using a 90° scattering angle. The latexes were diluted using deionised water that had been filtered through a 0.22 μm filter. The concentration was adjusted until the photon count rate at the detector was 100–200 kcounts s^{-1}.

Disk centrifuge photosedimentometry (DCP) measurements

The DCP measurements were carried out using a Brookhaven BI-DCP instrument. The spin fluid was prepared using the following procedure. Methanol 0.5 ml was injected into the stationary DCP disk via the injection port. Rotation of the disk was then started and water (15 ml) was injected in a steady stream within a time period of less than 3 sec. As soon as the disk had reached the set speed, dodecane (0.1 ml) was injected to form a barrier layer to methanol evaporation. The samples were prepared by adding a few drops of latex to a solution of methanol (0.1 ml) in deionised water (3 ml) in a glass vial, until a moderate turbidity was reached. The sample (0.2 ml) was then injected into the disk and the latex band passed through the laser detector within a period of a few minutes, the data being logged on a dedicated computer.

Transmission electron microscopy (TEM) analysis

The TEM samples from the latexes were prepared by diluting the latex in deionised water in a glass vial and dispersing the product in an ultrasonic bath for 5 min. A drop of the dispersion was deposited on a carbon-coated copper grid (Agar, 3.05 mm, 200 mesh), which was then placed on a filter paper and allowed to dry. The samples were examined using a Philips 400 EM transmission electron microscope, employing an accelerating voltage of 80 kV.

Results and discussion

Particle-size characterisation by DCP, TEM and PCS

Figure 2 shows transmission electron micrographs of the particles from the four latex suspensions. The products of all reactions showed narrow particle size distributions and, therefore, the images shown are representative of the products.

Table 2 summarises the number-average, weight-average and *z*-average diameters obtained from the DCP measurements. Fig. 3 shows the particle-size distributions obtained for sample R2, the particle-size distributions for the other samples are qualitatively similar. As can be seen, all latexes had narrow particle size distributions. The particle-size values obtained for the latexes R2 - R4 are slightly smaller than those reported by O'Callaghan et al. [7]. The particle sizes for the R3 and R4 latexes are close to the values calculated assuming that all newly-formed polymers add onto the seed particles, 763 nm for R3 and 1,334 nm for R4.

The mean particle sizes obtained from PCS for the products of reactions R1 and R2 were 100 and 480 nm. The slightly higher values compared to those obtained using DCP arise partly because PCS measures the hydrodynamic size of the particles, which includes the electrostatic double layer formed due to the presence of ionised groups on the surface of the particles. In addition, the average particle size obtained from PCS is the *z*-average diameter, whereas the diameters from DCP were number-average and weight-average values. For the latexes with larger particle sizes, i.e. R3 and R4, PCS did not give meaningful particle size averages (500 nm for R3 and 490 nm for R4) and the particle size distribution was bimodal or trimodal. This failure of PCS to measure meaningful sizes is not unexpected as the particle sizes of the R3 and R4 products are larger than the wavelength of the incident laser light (λ = 632 nm), hence the dipole scatterer approximation is not valid.

Table 2 Number-(d_n), weight-(d_w) and z-average (d_z) diameters from disc centrifuge photosedimentometry (DCP) measurements.

Latex	d_n(nm)	d_w (nm)	d_z (nm)	d_w/d_n
R1	85	90	94	1.06
R2	420	430	435	1.02
R3	734	740	747	1.01
R4	1,288	1,305	1,314	1.01

The uncertainties in the values are usually between 1 and 3%, as obtained by averaging the result of several measurements.

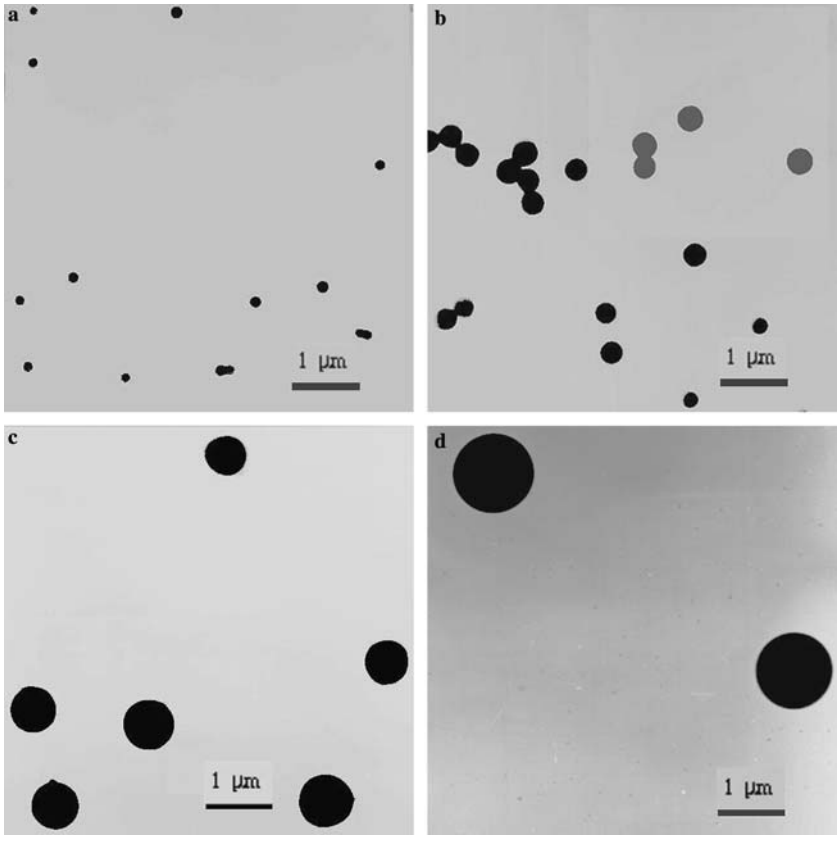

Fig. 2 Transmission electron micrographs of the products of **a** R1, **b** R2, **c** R3 and **d** R4 reactions. These images are only for illustration purposes, as no image analysis was performed on them

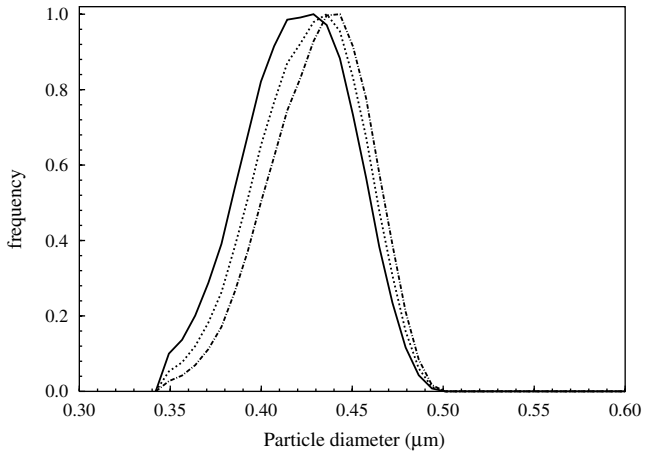

Fig. 3 Particle-size distributions obtained by DCP for the products of R2. Number-average (*solid line*), weight-average (*dashed line*) and z-average (*dashed dotted line*) distributions are presented. The particle-size distributions for the other three samples are qualitatively equivalent

Particle size characterisation using DWS

Figures 4 and 5 show the effect of concentration (at constant particle size) and particle size (at constant concentration) on DWS autocorrelation functions obtained from the measurements performed on the latex samples.

Figure 4 shows an increase of the decay rate of the ACF with concentration at constant size. This is expected as the scattering efficiency of the latexes increases with concentration, and there is also an increase in the viscosity of the latexes with concentration. This is apparent in the "flattening" of the tail of the ACF for the high-concentration samples. This effect is due to the restriction of the mean square displacement as the motion of the particles ceases to be Brownian [14].

A decrease in the decay rate of the ACF with increasing particle size at all concentrations studied was observed, as expected. This decrease is due to the slower motion of the larger particles leading to a slower degradation of the correlation. Fig. 5 shows the behaviour of the two extreme cases, the lowest and highest concentrations. As the concentration of the latex was increased, the ACFs of samples R1 and R2 became closer, until at volume fraction = 0.18 (Fig. 5), the correlograms for those two samples become indistinguishable. Hence it is not possible to use the ACF to determine a change in diameter in the size range of those two samples at high concentrations. This effect is shown in the plot of $\sqrt{\tau_0}/\gamma$ against d_z for the latexes (Table 3, Fig. 6).

Table 3 and Fig. 6 show that the values of the decay time of the ACF $\left(\sqrt{\tau_0}/\gamma\right)$ for the latexes prepared correlate well with the value of d_z obtained from DCP, and can be used for qualitative comparison of the particle sizes. In addition, as the volume fraction of the particles decreases, the sensitivity of the DWS technique to the change in the particle size increases. Calculation of particle size using Eq. 5 gives values that are far from those measured by DCP (see Table 4) because the assumption of high dilution (inherent in the derivation of Eq. 5) is not valid. However, as is evident from Fig. 6, it is possible to obtain calibration curves that could be used to facilitate measurements of particle size from the decay times $\left(\sqrt{\tau_0}/\gamma\right)$ of the DWS ACF. Since the purpose of the present work was to establish an analytical method for process control, the use of such calibration curves is appropriate. In these applications, the DWS decay times could be used to identify deviations from target particle sizes in monitoring of processes producing concentrated highly-scattering systems.

Fig. 4 DWS autocorrelation functions for the latexes at constant particle size for different volume fractions. The arrow indicates the direction of increasing concentration. **a** R1, **b** R4, at volume fractions 0.02 (*filled square*), 0.04 (*filled circle*), 0.09 (*filled triangle*) and 0.18 (*filled inverted triangle*). R2 and R3 show qualitatively similar behaviour

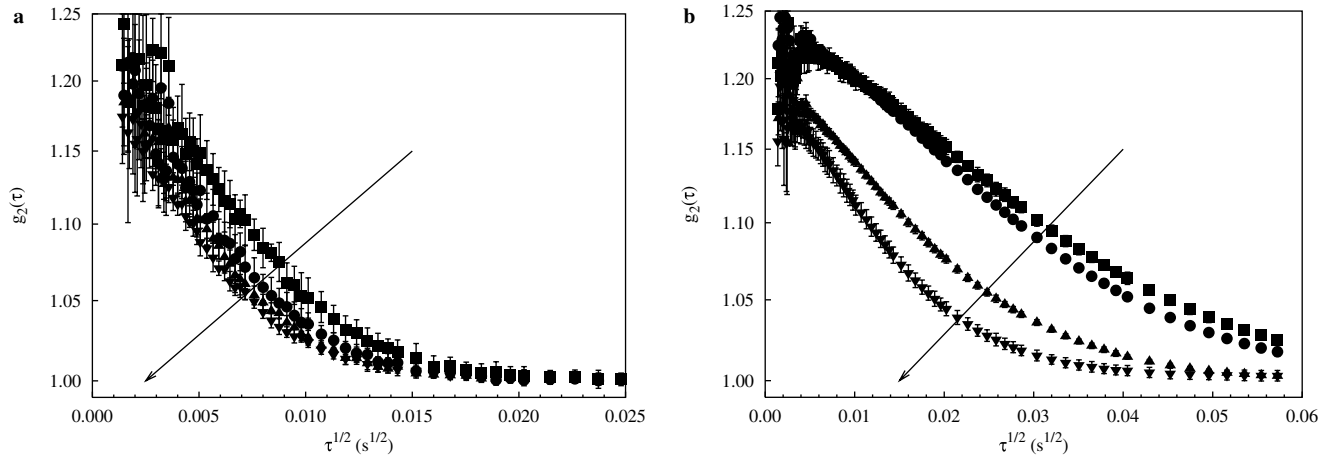

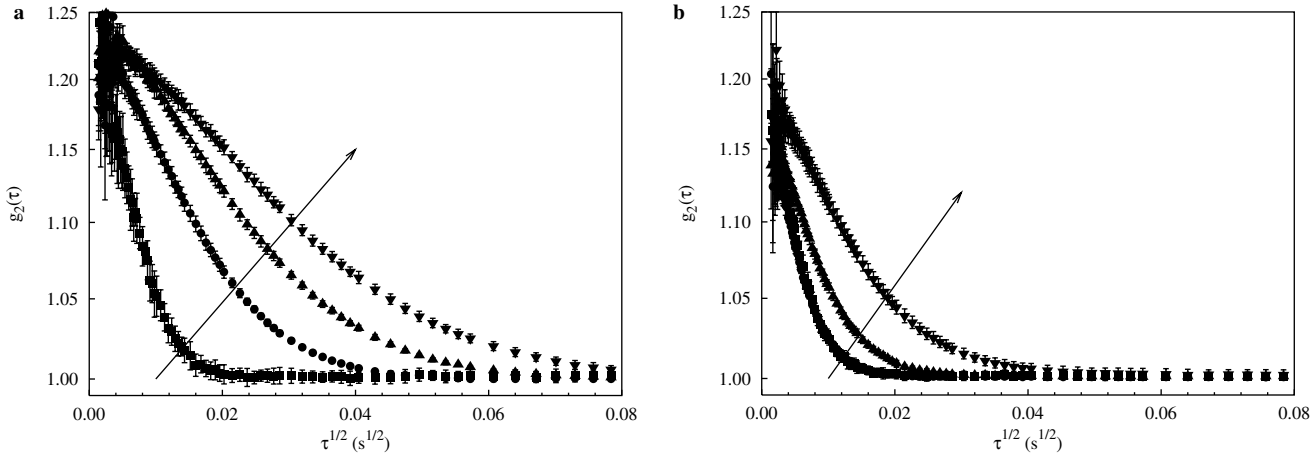

Fig. 5 DWS autocorrelation functions for the latexes at constant volume fraction for different particle sizes. The arrow indicates the direction of increasing size. **a** 0.02, **b** 0.18, with sizes: d_w = 90 nm (*filled square*); R2, d_w = 430 nm (*filled circle*); R3, d_w = 740 nm (*filled triangle*); R4, d_w = 1,305 nm (*filled inverted triangle*)

The effect of volume fraction on the sensitivity of the DWS technique is shown more clearly in Fig. 7, from which it is seen that the decay rate of the ACF decreases with concentration and approaches a limiting value as volume fraction increases. For the latexes with small particle sizes, R1 and R2, the decay times are close to the

Table 3 Decay times from DWS measurements against z-average particle diameter from DCP for latexes of different volume fractions (V_f).

d_z (nm)	$\sqrt{\tau_0}/\gamma(\times 10^{-2} s^{1/2})$			
	V_f= 0.02	V_f= 0.04	V_f= 0.09	V_f = 0.18
94	2.41 ± 0.01	2.02 ± 0.01	2.01 ± 0.01	2.24 ± 0.02
435	7.03 ± 0.05	4.89 ± 0.02	3.22 ± 0.01	2.42 ± 0.01
747	8.56 ± 0.10	7.76 ± 0.04	5.13 ± 0.02	3.82 ± 0.03
1,314	12.29 ± 0	14.85 ± 0	9.68 ± 0	7.04 ± 0

Table 4 Particle sizes calculated from the DWS measurements.

d_z (nm)	DWS size (nm)			
	V_f = 0.18	V_f = 0.09	V_f = 0.04	V_f = 0.02
94	109	49	22	30
435	148	139	137	268
747	352	342	339	393

R4 (d_z = 1,314 nm) was used to calculate γ for each of the concentrations, and therefore is not shown.

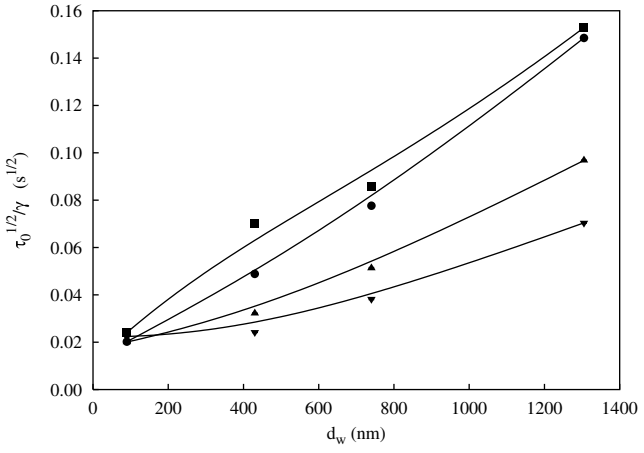

Fig. 6 Decay times of the DWS autocorrelation functions as a function of particle diameter at volume fractions of 0.02 (*filled square*), 0.04 (*filled circle*), 0.09 (*filled triangle*) and 0.18 (*filled inverted triangle*). The *solid lines* are drawn to indicate the trend.

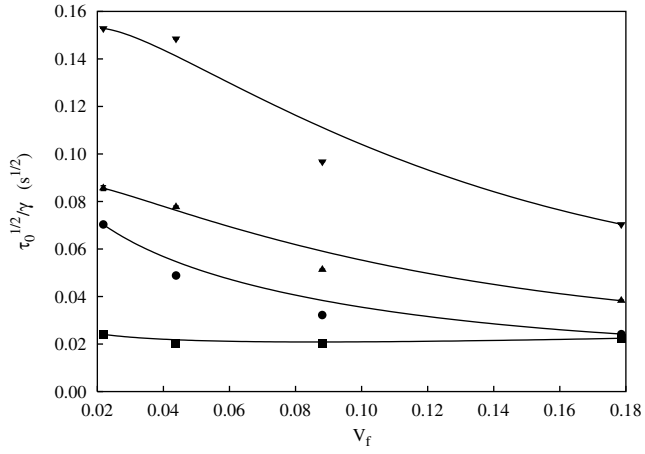

Fig. 7 Dependency of the DWS autocorrelation function decay rate on volume fraction, V_f, for each of the latexes: R1, d_w = 90 nm (*filled square*); R2, d_w = 430 nm (*filled circle*); R3, d_w = 740 nm (*filled triangle*); R4, d_w = 1,305 nm (*filled inverted triangle*). The *solid lines* are drawn to indicate the trend

limiting value of sensitivity and reach the limit at V_f = 0.18, a lower volume fraction than for the samples with larger particle sizes (R3 and R4). The effect of concentration on sensitivity may be explained by considering that as the concentration increases, the movement of the particles ceases to be Brownian, so that the phase changes observed in the scattered light are due to collective motions of the particles [15, 16]. For larger particles this effect is not observed, and the intensity fluctuations measured by the DWS technique are still correlated with the Brownian diffusion of the particles

Conclusions

The DWS technique was successfully used for qualitative comparison of the particle sizes in polymer latexes at concentrations much higher than normally used for light-scattering techniques such as PCS. The concentration dependence of the DWS results was investigated and it was observed that for polymer latexes with volume fractions 0.02, 0.04 and 0.09, the decay rate of the ACF decreased with increasing particle size. At V_f = 0.18, however, the correlograms for the smaller particles became indistinguishable and it was not possible to use the ACF to determine a change in size of the samples. This was explained in terms of the non-Brownian motion of the sub-micron particles at high concentrations. Hence, as the concentration is increased, the ability of DWS to discriminate particles of different sizes deteriorates in the sub-micron range, but remains reliable for larger particles. In addition, the small sample volume, relatively short measurement time and the modular design of the probe using optical fibres make the instrument of potential use for real-time monitoring of changes in the particle size during size-reduction processes.

Acknowledgements The development of the DWS equipment used in this work was funded by a CASE studentship from the EPSRC sponsored by Glaxo-SmithKline.

References

1. Chu, B (1990) Laser light scattering. basic principles and applications, 2nd edn. Academic, San Diego
2. Berne BJ, Pecora R (2000) Dynamic light scattering. with applications to chemistry, biology and physics. Dover, New York
3. Maret G, Wolf PE (1987) Z Phys B 65:409
4. Pine DJ, Weitz DA, Chaikin PM, Herbolzheimer E (1988) Phys Rev Lett 63:1747
5. Weitz DA, Pine DJ (1993) Diffusing-wave spectroscopy In: Brown W (ed) Dynamic light scattering, the method and some applications. Clarendon, Oxford, pp 652
6. Rega C, Lloyd CJ, Attwood D, Clarke D, Geraghty P (2001) App Opt 40:4204
7. O'Callaghan KJ, Paine AJ, Rudin A (1995) J Polym Sci Polym Chem Ed 33:1849
8. Frisken BJ (2001) App Opt 40:4087
9. Bevington PR, Robinson DK (2003) Data reduction and error analysis for the physical sciences. McGraw-Hill, New York
10. Horne DS, Davidson SN (1993) Colloids Surfaces A 77:1
11. Mazer NA (1985) In: Pecora R (ed) Dynamic light scattering: applications of photon correlation spectroscopy. Plenum, New York, pp 305
12. MacKintosh FC, Zhu JX, Pine DJ, Weitz DA (1989) Phys Rev B 40:9342
13. Rojas-Ochoa LF, Romer S, Scheffold F, Schurtenberger P (2002) Phys Rev E 65:051403
14. Mason TG, Weitz DA (1995) Phys Rev Lett 74:1250
15. Ladd AJC, Gang H, Zhu JX, Weitz DA (1995) Phys Rev Lett 74:318
16. Ladd AJC, Gang H, Zhu JX, Weitz DA (1995) Phys Rev E 52:6550